Next, the field was rotated slightly in order to separate the 1–2 lines of each complex until they were approximately 50 MHz apart. Echoes were then observed simultaneously in two different rutile dielectric cavity modes [Figure 4(b)].

CONCLUSIONS

It is apparent from the experimental study that "hole burning" does not keep one from obtaining a spin-echo frequency response which is a good replica of the input-pulse frequency response, even though the turning angle is as great as 120°. If this condition is satisfied, no frequency distortion is observed as the delay time is increased. For turning angles greater than 120°, however, the spectral reproducibility of the echo is greatly distorted. This places an upper limit on the dynamic range of the input pulses in any spin-echo delay line system.

In spite of the fact that the spin echo is a relatively narrow band phenomenon it is still possible to obtain simultaneous echoes at different frequencies with no distorting effect of one echo upon the other. With proper design of a rutile cavity and choice of crystal orientation relative to the applied magnetic field, the frequencies at which the cavity and the absorption lines are resonant can be predetermined. Signal processing is then feasible for discrete frequencies throughout the entire x-band.

ACKNOWLEDGMENT

The authors wish to acknowledge P. M. Pan for his support throughout the project.

JOURNAL OF APPLIED PHYSICS VOLUME 40, NUMBER 2 FEBRUARY 1969

Dislocation Velocity on the $\{\bar{1}2\bar{1}2\}\langle 1\bar{2}13\rangle$ Slip Systems of Zinc

R. C. BLISH, II

Bell Telephone Laboratories, Incorporated, Murray Hill, New Jersey 07974

AND

T. VREELAND, JR.

California Institute of Technology, Pasadena, California 91109

(Received 22 July 1968; in final form 25 October 1968)

Dislocation velocity on the $\{\bar{1}2\bar{1}2\}\langle 1\bar{2}13\rangle$ slip systems of zinc monocrystals was deduced from the rate of growth of slip bands. Near 77°K dislocation velocity is directly proportional to stress, and screw dislocations move more rapidly than edge dislocations. The difference between edge and screw dislocation velocity can be interpreted in two ways. The pre-exponential factors in a thermal activation model may differ by a factor 4 while the common activation energy is 0.21 eV, or the pre-exponential factors are the same, but the activation energy for edge dislocations (0.22 eV) exceeds that for screws by 5%. Other experiments will be required to establish the appropriate model. The authors favor the second alternative since extra activation energy might be needed to change the core structure of the edge dislocations (which lie on the basal planes) to make them glissile. Near room temperature, dislocation velocity decreases and cross-glide increases with increasing temperature. It is suggested that dragging dipoles and debris caused by their dissociation are responsible for the decrease in dislocation velocity. Finally, it is shown that the temperature dependence of both the yield strength and the plastic modulus is similar to the temperature dependence of the stress required to produce a constant dislocation velocity.

INTRODUCTION

It has been well documented that dislocation dynamics play a very important role in establishing the deformation behavior of crystals. The nonbasal slip behavior of single crystals of zinc (experiments in which basal slip has been minimized) constitutes a good example that macroscopic properties are difficult to interpret without at least some dislocation observations which give information about the microscopic mechanisms which are involved. The first identification of the important nonbasal slip systems at room temperature, namely $\{\bar{1}2\bar{1}2\}\langle 1\bar{2}13\rangle$, was accomplished by Bell and Cahn[1] and confirmed by Predvoditelev *et al.*[2] Earlier experiments by Gilman[3] showed that nonbasal deformation in zinc is characterized by a decreased yield stress and increased "plastic modulus" with increasing temperature. "Plastic modulus" as used by Gilman is the slope of the stress-strain curve

[1] R. L. Bell and R. W. Cahn, Proc. Roy. Soc. (London) **A239**, 494 (1957).
[2] A. A. Predvoditelev, G. V. Bushuyeva, and V. M. Stepanova, Phys. Metals Metallog. (U.S.A.) **14**, 44 (1962).
[3] J. J. Gilman, Trans. AIME J. Metals **203**, 206 (1955).

after yielding. Stofel and Wood[4] and Lavrent'yev *et al.*,[5] have corroborated some of Gilman's observations. However, the dislocation processes responsible for this behavior were not determined. Electron microscopy observations reported by Price[6] and recent work by Adams *et al.*[7] and Laurentyev *et al.*[8] constitute the existing knowledge of dislocation behavior on these slip systems in zinc.

The present investigation is concerned with the dislocation dynamics pertinent to nonbasal deformation of zinc. While the macroscopic plastic strain rate is proportional to the product of the dislocation velocity and the dislocation density, only the effects of dislocation velocity were investigated in this study. The effects of dislocation density were minimized by restricting the observations to specimens subjected to very small plastic strains. The dislocations near free surfaces of the specimens were observed before and after stress pulsing by chemical etch pitting and Berg–Barrett x-ray diffraction topographs. Measurements of the velocity of edge and screw oriented dislocations as a function of stress and temperature were made and compared to the temperature dependence of the stress–strain behavior.

EXPERIMENTAL TECHNIQUES

Large randomly oriented monocrystals of 99.999% zinc were grown by a modified Bridgeman technique. Great care in the cleavage, acid machining, and annealing operations were exercised in order to produce oriented test specimens of relatively low dislocation density. The test specimens were aligned for compression in the $\bar{a}$ direction. This stress state minimized the resolved shear stress upon the basal slip systems, imposed a large resolved stress on two of the $\{\bar{1}2\bar{1}2\}\langle 1\bar{2}13\rangle$ slip systems, and a smaller resolved stress on the other four pyramidal slip systems (Schmid factors of 0.417 and 0.104, respectively).

Compression load pulses directed along the $\bar{a}$ axis were produced by a rapid loading machine[9] with special compression load fixtures and provision for control of the temperature environment. A pad of low-modulus material was placed between the loading surfaces of the testing machine and the test specimen to insure a uniform stress state. Slip bands on the $(10\bar{1}0)$ and

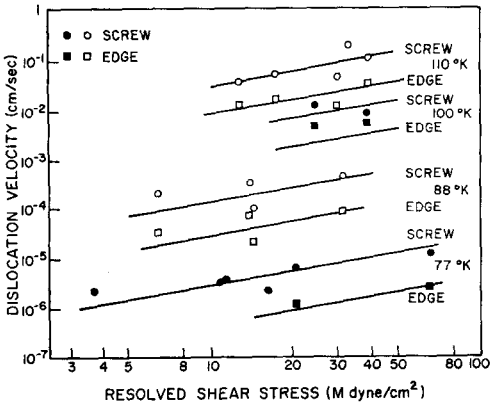

FIG. 1. Edge and screw dislocation velocity as a function of resolved shear stress, 77°–110°K.

$(10\bar{1}\ 24)$ surfaces of the specimens were observed by means of chemical etch pitting[10,11] after application of the stress pulse. The $(10\bar{1}\ 24)$ surfaces were also examined by means of Berg–Barrett x-ray diffraction topographs.[12]

The stress-strain curves at various temperatures were obtained from compression tests performed in an Instron testing machine using a cross-head speed of 0.00075 cm/min. Soft pads were also utilized in these tests to insure a uniform stress state.

EXPERIMENTAL RESULTS

Catastrophic failure of specimens by plastic buckling was observed at low temperatures and at normal stresses above 160 Mdyne/cm². Dislocation velocity data was obtained from specimens which did not buckle but developed slip bands as a result of the pulse loading.

Dislocation velocity was taken as the distance from the source of the slip band to its tip, divided by the duration of the stress pulse. The dislocation velocity data is shown in tabular form in Table I and in graphical form in Figs. 1, 2, and 3 as a function of resolved shear stress with absolute temperature and the edge or screw orientation as parameters. The straight lines in Fig. 1 resulted from the best fit to a model to be discussed later. Analysis of the loading and specimen geometry shows that observation of the two highly stressed slip bands on the $(10\bar{1}0)$ surface is related to the movement of pure edge dislocations, while the dislocations observed on $(10\bar{1}\ 24)$ are nearly pure screw dislocations (only 6° off). The corresponding angles for the four slip systems with the smaller Schmid

[4] E. J. Stofel and D. S. Wood, *Fracture of Solids*, J. B. Newkirk and J. H. Wernick, Eds. (Interscience Pub., New York, 1963), p. 521.
[5] F. F. Lavrent'yev, O. P. Salita, and V. I. Startsev, Phys. Metals Metallog. (U.S.A.) **10**, 95 (1966).
[6] P. B. Price, *Electron Microscopy and Strength of Crystals*, G. Thomas and J. Washburn, Eds. (Interscience Pub., New York, 1963), p. 41.
[7] K. H. Adams, R. C. Blish, II, and T. Vreeland, Jr., Mat. Sci. Eng. **2**, 201 (1967).
[8] F. F. Lavrentyev, O. P. Salita, and V. L. Vladimirova, Phys. Status Solidi **29**, 569 (1968).
[9] T. L. Russell, D. S. Wood, and D. S. Clark, Acta Met. **9**, 1054 (1961).
[10] R. G. Brandt, K. H. Adams, and T. Vreeland, Jr., J. Appl. Phys. **34**, 591 (1963).
[11] K. H. Adams, R. C. Blish, II, and T. Vreeland, Jr., J. Appl. Phys. **37**, 4291 (1966).
[12] D. P. Pope, T. Vreeland, Jr., and D. S. Wood, J. Appl. Phys. **38**, 4011 (1967).

TABLE I. Dislocation velocity measurements.

Temperature (°K)	Normal stress (Mdyn/cm²)	Resolved shear stress (Mdyn/cm²)	Edge dislocation velocity (cm/sec)	Screw dislocation velocity (cm/sec)
77	36.4	3.6	···	2.0×10^{-6}
77	104	10.8	···	3.2×10^{-6}
77	109	11.3	···	3.5×10^{-6}
77	157	16.3	···	2.2×10^{-6}
77	49.8	20.7	1.1×10^{-6}	6.3×10^{-6}
77	157	65.5	2.7×10^{-6}	1.3×10^{-5}
88	59.6	6.2	3.3×10^{-5}	2.0×10^{-4}
88	33.2	13.8	7.1×10^{-5}	3.3×10^{-4}
88	34.4	14.3	2.0×10^{-5}	1.0×10^{-4}
88	74.1	30.9	8.8×10^{-5}	4.6×10^{-4}
100	57.7	24.0	4.8×10^{-3}	1.3×10^{-2}
100	90.6	37.7	5.7×10^{-3}	9.6×10^{-3}
110	30.0	12.5	1.3×10^{-2}	4.0×10^{-2}
110	41.1	17.1	1.8×10^{-2}	5.8×10^{-2}
110	69.8	29.0	1.3×10^{-2}	5.1×10^{-2}
110	76.7	31.9	···	2.1×10^{-1}
110	91.1	37.9	3.8×10^{-2}	1.2×10^{-1}
175	35.4	14.7	8.4×10^{-2}	2.8×10^{-1}
175	73.0	30.4	2.5×10^{-1}	···
200	20.4	8.6	1.3×10^{-2}	6.3×10^{-2}
200	25.7	10.7	3.3×10^{-2}	5.1×10^{-2}
200	40.1	16.7	8.8×10^{-2}	4.6×10^{-2}
200	53.9	22.4	3.3×10^{-1}	7.4×10^{-1}
200	74.5	31.0	5.1×10^{-1}	1.4
230	28.2	11.7	6.1×10^{-2}	6.1×10^{-2}
230	59.6	24.8	1.8×10^{-1}	3.5×10^{-1}
273	21.6	9.0	4.3×10^{-3}	5.8×10^{-3}
273	28.4	11.8	5.8×10^{-2}	6.7×10^{-2}
273	40.3	16.8	3.0×10^{-1}	3.3×10^{-1}
273	45.1	19.2	6.0×10^{-1}	···
273	57.0	23.3	6.8	$1.5\times10^{+1}$
294	18.9	7.9	2.5×10^{-4}	···
294	24.8	10.3	2.0×10^{-3}	1.5×10^{-3}
294	27.4	11.4	6.1×10^{-3}	···
294	29.8	12.4	5.6×10^{-3}	7.1×10^{-3}
294	32.7	13.6	1.0×10^{-2}	···
294	39.2	16.3	4.1×10^{-2}	···
294	53.9	22.4	5.6×10^{-1}	···
294	58.0	24.1	3.8×10^{-1}	···
294	69.7	29.0	1.0	···
294	70.5	29.3	8.1	5.8
294	74.5	31.0	7.6	···
323	56.3	23.4	4.5×10^{-5}	···
323	58.2	24.2	5.1×10^{-4}	7.1×10^{-4}
323	66.1	27.5	2.8×10^{-2}	2.8×10^{-2}
323	75.3	31.3	2.8×10^{-1}	2.8×10^{-1}
323	76.0	31.6	1.9×10^{-2}	1.9×10^{-2}
323	86.1	35.8	3.0	3.0

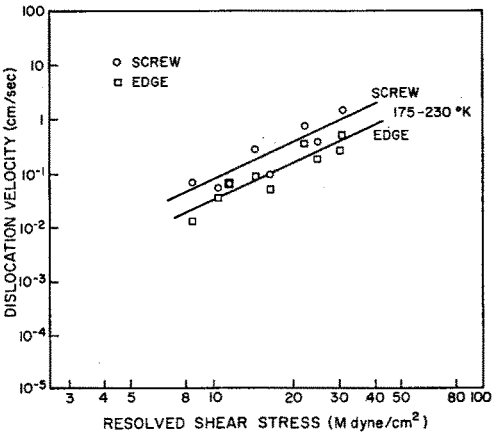

FIG. 2. Edge and screw dislocation velocity as a function of resolved shear stress, 175°–230°K.

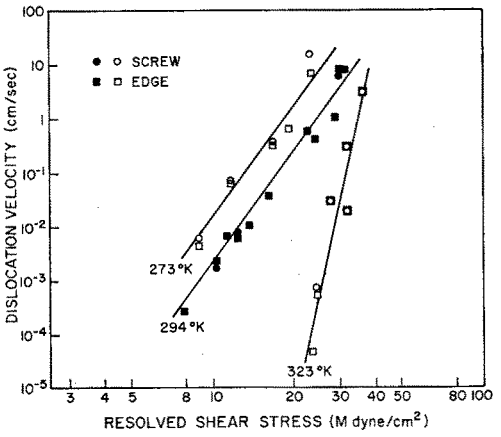

FIG. 3. Edge and screw dislocation velocity as a function of resolved shear stress, 273°–323°K.

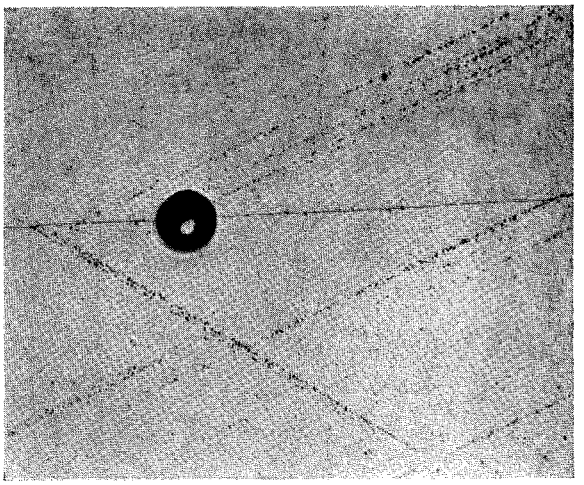

FIG. 4. $(10\bar{1}0)$ surface, $\bar{a}$ vertical, slip bands formed at 200°K, 22.4 Mdyne/cm², 0.610 sec, 1.27×1.53 mm field.

factor are: 38° off pure edge for dislocations seen on $(10\bar{1}0)$ and only 3° off pure screw for the $(10\bar{1}\,24)$.

Changes in the morphology of the slip bands were observed as a function of temperature. Over the range 77°–200°K the slip bands have very little width indicating a relatively small amount of cross-glide. In addition, all the slip bands were single-ended, most having been nucleated at small-angle tilt boundaries. Figure 4 shows narrow slip bands nucleated at the small-angle boundary on an etch-pitted $(10\bar{1}0)$ surface. The slip bands were formed by a stress pulse of 53.7 Mdyne/cm² for 0.61 sec (22.4 Mdyne/cm² resolved shear stress) at a temperature of 200°K. Wider, tapered slip bands are observed on etch-pitted $(10\bar{1}0)$ surfaces in Figs. 5 and 6 at temperatures of 273° and 323°K, respectively. The slip bands were formed by stress pulses of 40.3 Mdyne/cm² (16.8 Mdyne/cm² resolved), 1.56 sec, and 85.8 Mdyne/cm² (35.8 Mdyne/cm² resolved), 0.109 sec, respectively. Although, it is not

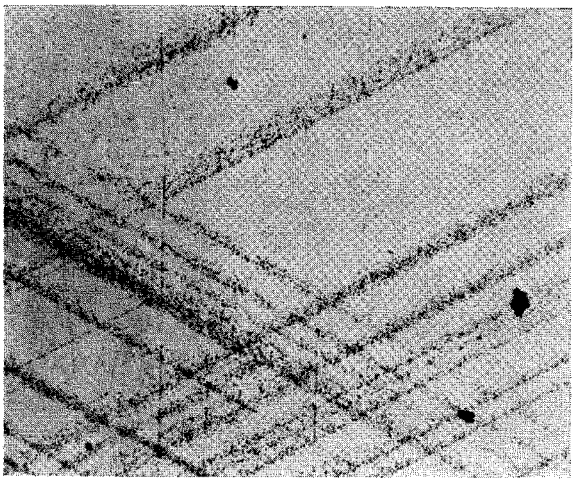

FIG. 5. $(10\bar{1}0)$ surface, $\bar{a}$ vertical, slip bands formed at 273°K, 16.8 Mdyne/cm², 1.56 sec, 1.27×1.53 mm field.

evident in these two photomicrographs, these slip bands are tapered and many of them are symmetrical and appear to have formed from a surface source which was not associated with a small angle boundary.

The slip bands seen on the $(10\bar{1}\,24)$ face are broader than those observed on $(10\bar{1}0)$, as one might expect since the former are comprised of screw dislocations which are able to cross-glide, in contrast to the edge dislocations seen on the $(10\bar{1}0)$ face. The screw oriented slip bands have nearly the same width along their length, as opposed to the taper in width seen on the $(10\bar{1}0)$ face. Figure 7 shows an etch-pitted $(10\bar{1}\,24)$ surface exhibiting these features. The slip bands were formed by a stress pulse of 58.0 Mdyne/cm² (24.2 Mdyne/cm² resolved), 300 sec, at a temperature of 323°K.

Figure 8 illustrates the correspondence between an x-ray diffraction topograph and the same $(10\bar{1}\,24)$

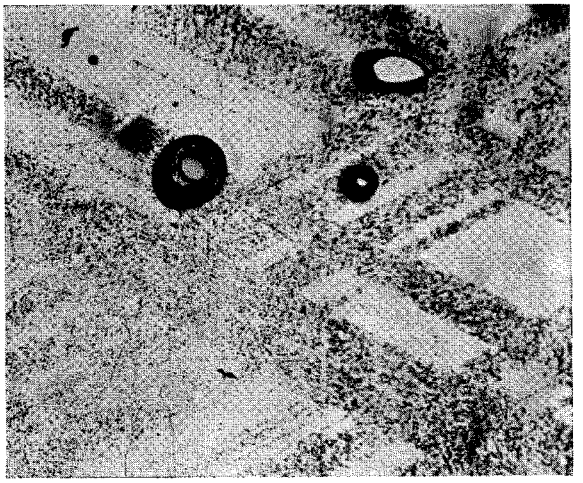

FIG. 6. $(10\bar{1}0)$ surface, $\bar{a}$ vertical, slip bands formed at 323°K, 35.8 Mdyne/cm², 0.109 sec, 1.27×1.53 mm field.

surface after etch-pitting. Low-angle boundaries can be seen in both pictures and the slip bands were formed by a stress pulse of 74.4 Mdyne/cm² (31.0 Mdyne/cm² resolved), 0.346 sec at a temperature of 200°K. At a greater magnification the individual dislocations making up the slip bands can just be resolved in the x-ray topograph.

Figure 9 shows an x-ray topograph in which basal dislocations, which are nearly parallel to the $(10\bar{1}\,24)$ observation surface, have been impeded by what is probably a pyramidal slip band. Pyramidal dislocations constitute a forest for basal dislocations, and there is the possibility of attractive junctions between the two species. Furthermore, the trace of the forest which impeded the basal dislocations corresponds to the trace of one of the nonbasal slip systems with a low Schmid factor. These bands were formed by a pulse of 36 Mdyne/cm² (3.6 Mdyne/cm² resolved), 1.5×10^5 sec at a temperature of 77°K.

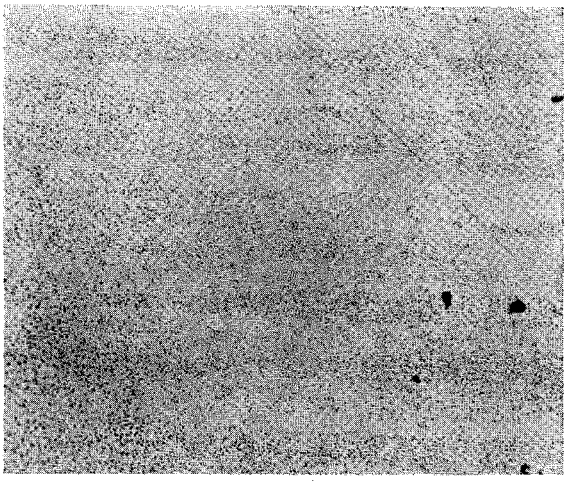

FIG. 7. $(10\bar{1}\,24)$ surface, $\bar{a}$ vertical, slip bands formed at 323°K, 24.2 Mdyne/cm², 300 sec, 1.27×1.53 mm field.

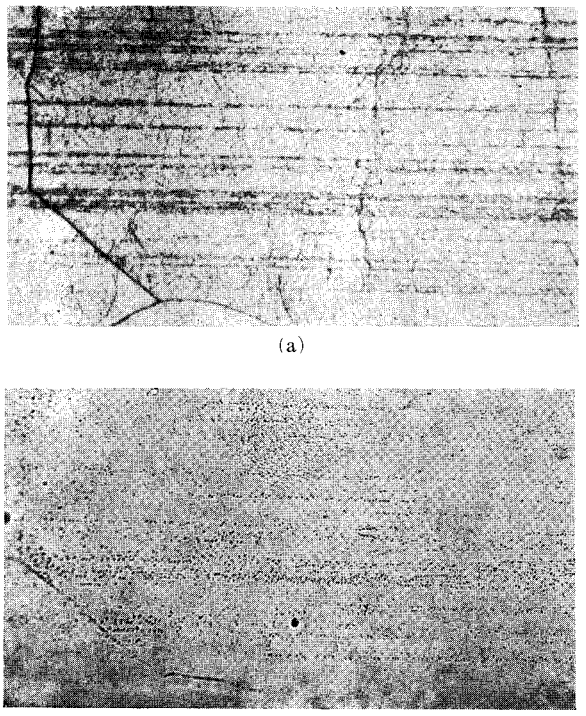

(a)

(b)

FIG. 8. $(10\bar{1}\,24)$ surface, $\bar{a}$ vertical, slip bands formed at 323°K, 24.2 Mdyne/cm², 0.346 sec, 0.89×1.53 mm field, (a) x-ray micrograph, (b) etched surface.

The 0.01% offset yield stress as a function of temperature was obtained from stress–strain curves and is shown in Fig. 10 with other data to be explained later. The plastic modulus as a function of temperature is shown in Fig. 11. Increasing yield strength at low temperatures, and increasing plastic modulus at high temperatures were also reported by Gilman.[3]

FIG. 9. $(10\bar{1}\,24)$ surface, $\bar{a}$ horizontal, x-ray micrograph showing basal dislocations interacting with pyramidal slip bands, 1.27×1.53 mm field.

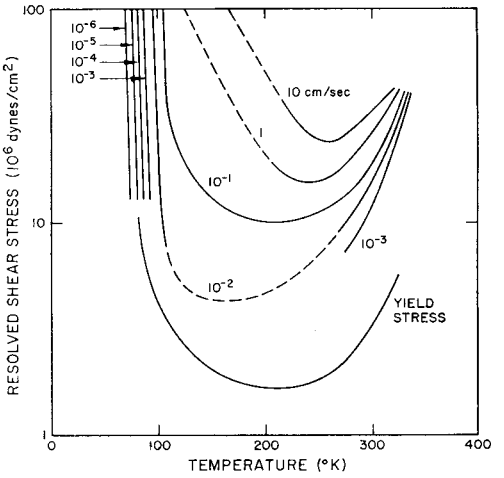

FIG. 10. Constant dislocation velocity contours as a function of stress and temperature, and the 0.01% offset yield strength for $\{\bar{1}2\bar{1}2\}\langle 1\bar{2}13\rangle$ slip in zinc.

DISCUSSION

The variation in dislocation velocity from one test to another on the same crystal or from one crystal to another was found to be about ±20%. This variation is large compared to the ±1% errors in measurement of stress and time. The temperature measurements were accurate to about ±2°K and since dislocation velocity is quite sensitive to temperature, inaccurate temperature control can account for some of the ob-

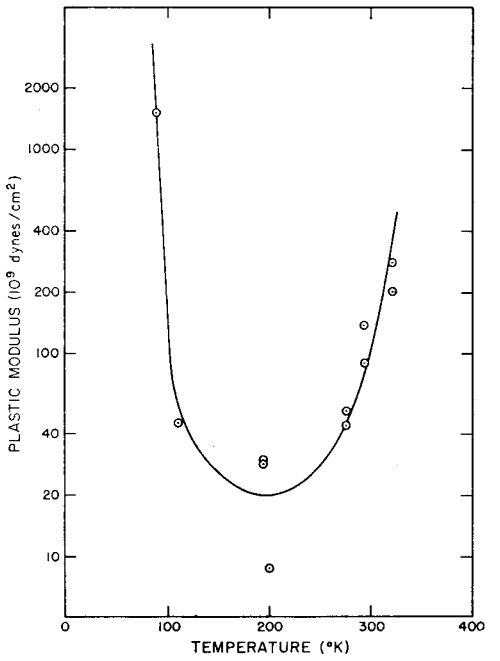

FIG. 11. Plastic modulus as a function of temperature for $\{\bar{1}2\bar{1}2\}\langle 1\bar{2}13\rangle$ slip in zinc.

served variation. However, most of the variation is attributed to differences in dislocation density and substructure in the crystals. Previous investigators have noted the structure-sensitivity of the plastic properties of zinc crystals. For example, we have found that the twinning behavior of zinc is structure-sensitive.[13] Lavrent'yev and Salita[14] found that the "starting stress" for pyramidal slip in zinc varies by a factor of 2–3 between crystals having different amounts of substructure. We have discussed elsewhere the significance of their "starting stress" in light of dislocation velocity.[15] Dislocation velocity data vs stress at room temperature presented in this work, has essentially the same functional form as the work reported by Adams *et al.*,[7] except the stress levels differ by a factor of about 2. Adams' crystals possessed a greater dislocation density than the crystals used in this work (10^5–10^6 cm^{-2} vs 10^3–10^5 cm^{-2}) which probably accounts for the increased stress required to produce the same dislocation velocity.

It can be seen in Fig. 1 that the screw dislocations move faster than edge dislocations for a given stress and temperature near 77°K. Furthermore, the ratio of screw dislocation velocity to that of the edge dislocations decreases with increasing temperature. It can also be seen in Fig. 1 that dislocation velocity is directly proportional to resolved shear stress. These characteristics of the dislocation velocity measurements led us to fit the data to the following mathematical model

$$v_e = A\tau \exp(-U_e/kT)$$

$$v_s = A\tau \exp(-U_s/kT),$$

where v is the dislocation velocity, A is a proportionality constant, τ is the resolved shear stress, U is the activation energy, k is Boltzmann's constant, T is the absolute temperature, and e and s are subscripts pertaining to edge and screw orientations respectively. A least-squares fit of the data (77°–110°K) to the model yields the following values for the parameters:

$$A = 10 \text{ (cgs)}; \qquad U_e = 0.218 \text{ eV}; \qquad U_s = 0.207 \text{ eV}.$$

A graphical illustration of the fit of the data to this model is shown in Fig. 12, in which average values of $\log_{10} v/\tau$ are plotted against $1/T$ (estimated experimental errors are given by the vertical bars). The slope is related to the activation energy, and the pre-exponential factor A is the same for both screw and edge dislocations.

The data can also be fitted to a model in which edge and screw dislocations have the same activation energy but different pre-exponential factors. Using the same notation the mathematical model is

$$v_e = A_e\tau \exp(-U/kT)$$

$$v_s = A_s\tau \exp(-U/kT).$$

A least-squares fit to this model yields the following values for the parameters:

$$A_e = 4.1 \qquad A_s = 17.1 \qquad U = 0.211 \text{ eV}.$$

The standard deviation, defined as the rms value of $\log_{10}(v/v_{\text{calc}})$, and the product-moment correlation coefficient were identical for the two models. The standard deviation was 0.20, a factor of 1.6, of which about $\frac{1}{3}$ is the random measurement error. The correlation coefficient was 0.88, which implies a Fisher's Z of 1.38. The standard error in Z was 0.20, a very good correlation for either of the models.

The data can be equally well fitted to an equation of the form

$$v = A \exp(-U/kT + \gamma b\tau/kT),$$

where γ is an activation area and b is the Burgers vector (5.6 Å). The numerical value of γ is about $1.7b^2$ from 77°–110°K. The range of the stress–velocity data is not sufficient to indicate which of the three functional forms give the best fit, but the authors favor the first one for reasons to be discussed later.

The measurement of the velocity of "screw" dislocations near 77°K underestimates the actual velocity of pure screw dislocations because there is slight mis-

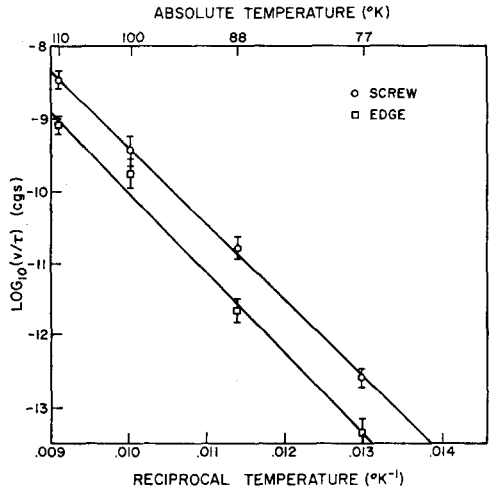

FIG. 12. Plot of $\log v/\tau$ vs $1/T$ for edge and screw dislocations on the $\{\bar{1}2\bar{1}2\}\langle 1\bar{2}13\rangle$ slip system of zinc, temperature range 77°–110°K. Bars denoted estimated errors in the experimental values.

[13] R. C. Blish, II, and T. Vreeland, Jr., Phil. Mag. **17**, 849 (1968).
[14] F. F. Lavrent'yev and O. P. Salita, Sov. Phys. Doklady (U.S.A.) **8**, 803 (1964).
[15] R. C. Blish, II, and T. Vreeland, Jr., J. Appl. Phys. **39**, 2816 (1968).

orientation of the observation surface from the basal plane where pure screw dislocations would be observed. Assuming that a dislocation loop grows into an ellipse on the slip plane, the pure screw dislocations will be characterized by a velocity about 10% greater than the velocity actually observed. However, this increment is less than the scatter in the experimental measurements so the misorientation was neglected.

We assume that in the temperature range 77°K–110°K, the Peierls barrier controls dislocation motion. The data indicate that the activation energy for formation of a double kinks on edge dislocations might exceed that for screw dislocations by about 5%. This could be due to a difference in kink energies on edge and screw dislocations, and/or to a difference in core structure. There is evidence that the core of the edge dislocation might be spread on the basal plane or fully dissociated into sessile partial dislocations.[6] The screw dislocation, which does not lie in the basal plane, will most likely not exhibit such an asymmetric core structure. The spread core or dissociated edge dislocations would then require more energy than the screw dislocations in order to constrict sufficiently for the formation of a double kink. The authors feel that the 5% difference in activation energies is a more likely interpretation than a factor of 4 difference in the pre-exponential factors, so the first model is preferred.

The data deviate from the linear relationship shown in Fig. 12 for temperatures above 110°K. The morphology of the slip bands also changes for temperatures above 200°K. In addition, it can be seen in Fig. 3 that above about 200°K the dislocation velocity actually decreases with increasing temperature for a given stress. This implies a negative activation energy in the formulations of the velocity–stress relationship which we have discussed. All of these considerations indicate that the mechanism which governs the dislocation velocity has changed from that which was acting near 77°K.

Price[6] has observed extensive production of dislocation dipoles on the pyramidal slip systems of zinc at temperatures as low as about 100°K. These dipoles were observed to break up into dislocation loops rather rapidly near room temperature. The dipoles constitute an additional drag working against the movement of the leading dislocation of a slip band, and the loops produced by dissociation of the dipoles should effectively obstruct the dislocations which follow. The leading dislocation in a slip band may therefore move ahead of the visible slip band which is obstructed by the dipole debris. We believe that the slip-band growth observed in this study at the higher temperatures is limited by the motion of dislocations through the debris left behind by the leading dislocation. The decreasing velocity with increasing temperatures above 200°K is attributed to an increasing amount of cross-glide and an increasing rate of dipole dissociation into debris loops.

The dislocation-velocity contours (mean of edge and screw velocity) are presented in Fig. 11 as a function of temperature and resolved shear stress together with the resolved stress required to produce 0.01% plastic strain. It can be seen that the iso-velocity contours and the yield stress have the same temperature dependence. The is an indication that the dislocation velocity is strongly affecting the macroscopic yield stress.

Dislocation velocity also has a strong effect upon the apparent plastic modulus (see Fig. 11). Its sharp increase for temperatures below 100° and above 300°K is attributed to the fact that dislocation velocity, and, therefore, the plastic strain rate, drops sharply in those temperature regions.

CONCLUSIONS

(1) Dislocation velocity on the $\{\bar{1}2\bar{1}2\}\langle 1\bar{2}13\rangle$ slip systems of zinc is characterized by a thermally activated process and a linear proportionality to stress for the temperature range 77°K–110°K.

(2) Edge and screw dislocation velocities may be characterized by the same pre-exponential factor and different activation energies, namely, $U_e=0.218$ eV and $U_s=0.207$ eV for the temperature range 77°K–110°K. An alternative analysis less favored by the authors indicates that the pre-exponential factor for screw dislocation exceeds that for edge dislocations by a factor of 4, and the common activation energy is 0.211 eV. It is suggested that the Peierls forces control the dislocation velocity in this temperature range.

(3) Above 110°K dislocation velocity is governed by a different mechanism whose most important manifestations are increased cross-glide and a decrease in dislocation velocity with increasing temperature. In this temperature range the dislocation velocity is thought to be influenced by the drag exerted by dipoles which are produced in greater numbers by increased cross-glide.

(4) The temperature dependence of the yield strength and the apparent plastic modulus is controlled by the temperature dependence of dislocation velocity.

ACKNOWLEDGMENTS

The authors wish to express their appreciation to the U.S. Atomic Energy Commission who sponsored this investigation. The assistance of G. R. May and R. L. Norton in specimen preparation and testing is gratefully acknowledged.